

Synthesis, characterization and reactivity of linear-type S-bridged trinuclear complexes containing vanadium(III) ion. Crystal structures of $[V^{III}\{M(aet)_3\}_2](ClO_4)_3$ ($M = Rh^{III}, Ir^{III}$; $aet = 2\text{-aminoethanethiolate}$)[†]

Yoshitaro Miyashita,* Masato Hamajima, Yasunori Yamada, Kiyoshi Fujisawa and Ken-ichi Okamoto*

Department of Chemistry, University of Tsukuba, Tsukuba 305-8571, Japan.
E-mail: okamoto@chem.tsukuba.ac.jp

Received 1st March 2001, Accepted 22nd May 2001

First published as an Advance Article on the web 26th June 2001

Reactions of $fac(S)\text{-}[M(aet)_3]$ ($M = Rh^{III}, Ir^{III}$; $aet = 2\text{-aminoethanethiolate}$) with an excess of VCl_3 gave linear-type S-bridged trinuclear complexes $[V^{III}\{M(aet)_3\}_2]^{3+}$ ($M = Rh^{III}$ **1**, Ir^{III} **2**). The $\Delta\Lambda$ isomers (**1a**(ClO_4)₃ and **2a**(ClO_4)₃) were selectively crystallized and their structures were determined by X-ray diffraction. Both the complex cations consist of two terminal $fac(S)\text{-}[M(aet)_3]$ units and a central vanadium atom, which is situated in an octahedral environment with a $V^{III}S_6$ chromophore. The Ir complex **2a** was also formed by using $V^{IV}OCl_2$ instead of $V^{III}Cl_3$ in a redox reaction, whereas the Rh complex **1a** was not formed by a similar method. The optically active isomer ($\Delta\Lambda$ -**1b**) of the Rh complex was selectively obtained by using $\Lambda\text{-}fac(S)\text{-}[Rh(aet)_3]$, and characterized by IR, UV-VIS absorption and CD spectra. All the obtained complexes exhibit a unique strong absorption band at $ca. 18 \times 10^3 \text{ cm}^{-1}$. Stability and reactivity relating to V–S bond cleavage for the complexes were investigated using UV-VIS absorption spectroscopic methods. These studies show first order decomposition or metal exchange. While **2a** has weaker V–S bonds than **1a** (from the X-ray analyses), the former is considerably more stable in water than the latter. Cyclic voltammograms of **1a** and **2a** in water show only irreversible oxidation and reduction waves including $V^{IV/III}$ and $V^{III/II}$ processes. The $V(III)$ ions in the S-bridged trinuclear structures exhibit a lower magnetic moment ($2.59 \mu_B$ for **1a** and $2.27 \mu_B$ for **2a**) at room temperature than the spin-only value for a d^2 electronic configuration.

Introduction

Vanadium/sulfur chemistry has been studied mainly with regard to the vanadium nitrogenase system¹ and refining of crude oils;² vanadium compounds such as sulfide clusters have been extensively investigated. On the other hand, it is well known that ascidians accumulate $V(III)$ ion (the instability of which under aerobic conditions is recognized) to a great extent in their blood cells from sea water selectively.³ Recently, it has been reported that vanadium associated proteins in the ascidians contain cysteine,⁴ and thus some important interactions between $V(III)$ ions and sulfur atoms are anticipated. However, studies on sulfur-containing $V(III)$ complexes are still rare, since vanadium usually exists as more stable vanadyl ($V(IV)$) or vanadate ($V(V)$) species, which have $V=O$ unit(s). Moreover, the $V(III)$ ion can adopt various coordination geometries, e.g. $V(III)$ ion in dinuclear complexes with alkoxo bridges adopts hexa-coordinated octahedral or hepta-coordinated capped trigonal prismatic structure depending on the stereochemistry of the polydentate ligands.⁵ Hence, control of coordination geometry as well as stabilization of the lower oxidation state by suitable ligands are required in order to explore fundamental properties of sulfur-containing $V(III)$ complexes.

It has been recognized that the tridentate metalloligands $fac(S)\text{-}[M(aet)_3]$ ($M = Cr^{III}, Co^{III}, Rh^{III}, Ir^{III}$; $aet = 2\text{-aminoethanethiolate}$) react with a variety of metal ions to form the S-bridged polynuclear complexes.⁶ Among them, Rh and Ir complexes, which have stronger M–S bonds than Cr and

Co complexes, are suitable as building blocks for selective construction of polynuclear structures. Indeed, we reported recently that the metalloligands $fac(S)\text{-}[M(aet)_3]$ ($M = Rh^{III}, Ir^{III}$) can incorporate early transition metal ions to form the S-bridged polynuclear complexes, in which the metalloligands retain their octahedral $fac(S)$ structures.^{7–9} These complexes containing the octahedral $Cr(III)$,⁷ $Mo(III,IV)$ ⁸ or $Re(III)$ ⁹ ions showed unique reactivity, electrochemistry and magnetic properties due to the relatively weak affinity of these metal ions toward thiolato-sulfur atoms and electromagnetic interactions in the polynuclear structures by unpaired d electrons in the t_{2g} orbitals. In these S-bridged polynuclear structures, it can be considered that relatively low oxidation states ($Mo(III,IV)$, $Re(III)$) are stabilized by the $fac(S)\text{-}[M(aet)_3]$ units. Furthermore, since the metalloligands have only weak absorption bands in the visible region,^{6–15} spectrochemistry of the metal ions incorporated into the polynuclear structures can be investigated clearly.

In this work, linear-type S-bridged trinuclear complexes $[V\{M(aet)_3\}_2]^{3+}$ containing $V(III)$ were newly prepared using the stable metalloligands $fac(S)\text{-}[M(aet)_3]$ ($M = Rh^{III}, Ir^{III}$). Their structures were determined by X-ray diffraction. Spectral properties were discussed in terms of their IR, UV-VIS absorption and CD spectra. Further, the stability and reactivity of the present complexes concerning weak V–S bonds are also discussed in detail. The redox and magnetic properties were also investigated.

Results and discussion

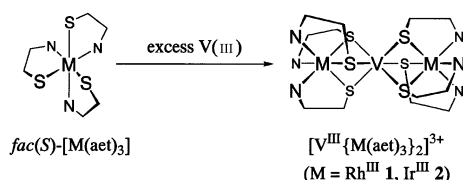
Formation of complexes

The reaction of $fac(S)\text{-}[M(aet)_3]$ ($M = Rh^{III}, Ir^{III}$) with a large excess of VCl_3 in water gave the linear-type S-bridged trinuclear

[†] Electronic supplementary information (ESI) available: Fig. S1 Absorption spectral change of $\Delta\Lambda\text{-}[V\{Rh(aet)_3\}_2]^{3+}$ (**1a**) upon addition of $Co(II)$; the curves show the spectra measured at 5 min intervals. See <http://www.rsc.org/suppdata/dt/b1/b101965/>

Table 1 Selected bond distances (Å) and angles (°) for $\Delta\Lambda$ -[V{Rh(aet)₃}₂]³⁺ (**1a**) and $\Delta\Lambda$ -[V{Ir(aet)₃}₂]³⁺ (**2a**)

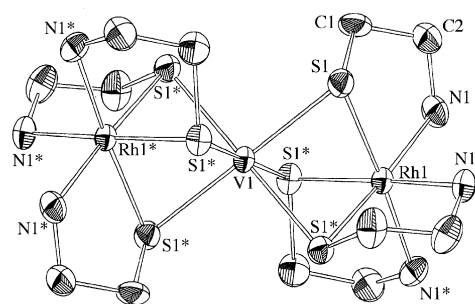
Complex 1a							
Rh(1)–S(1)	2.318(3)	S(1)–Rh(1)–N(1)	86.0(3)	S(1)–Rh(1)–S(1)*	90.12(9)	S(1)–V(1)–S(1)*	94.50(8)
Rh(1)–N(1)	2.119(8)	S(1)–Rh(1)–N(1)*	88.9(3)	N(1)–Rh(1)–N(1)*	94.9(3)	S(1)–V(1)–S(1)*	180.0
V(1)–S(1)	2.416(2)	S(1)–Rh(1)–N(1)*	176.0(3)	Rh(1)–S(1)–V(1)	73.56(8)	S(1)–V(1)–S(1)*	85.53(8)
Rh(2)–S(2)	2.329(3)	S(2)–Rh(2)–N(2)	86.3(4)	S(2)–Rh(2)–S(2)*	90.7(1)	S(2)–V(2)–S(2)*	93.9(1)
Rh(2)–N(2)	2.08(1)	S(2)–Rh(2)–N(2)*	90.4(4)	N(2)–Rh(2)–N(2)*	92.7(4)	S(2)–V(2)–S(2)*	180.0
V(2)–S(2)	2.427(3)	S(2)–Rh(2)–N(2)*	176.8(4)	Rh(2)–S(2)–V(2)	72.76(9)	S(2)–V(2)–S(2)*	86.1(1)
Rh(2)–S(3)	2.32(2)	S(3)–Rh(2)–N(3)	84(1)	S(3)–Rh(2)–S(3)*	91.6(5)	S(3)–V(2)–S(3)*	94.4(5)
Rh(2)–N(3)	2.18(4)	S(3)–Rh(2)–N(3)*	86(1)	N(3)–Rh(2)–N(3)*	97(1)	S(3)–V(2)–S(3)*	180.0
V(2)–S(3)	2.45(1)	S(3)–Rh(2)–N(3)*	175(1)	Rh(2)–S(3)–V(2)	72.5(4)	S(3)–V(2)–S(3)*	85.6(5)
Complex 2a							
Ir(1)–S(1)	2.326(3)	S(1)–Ir(1)–N(1)	84.7(3)	S(1)–Ir(1)–S(1)*	92.0(1)	S(1)–V(1)–S(1)*	93.3(1)
Ir(1)–N(1)	2.1269(9)	S(1)–Ir(1)–N(1)*	87.9(3)	N(1)–Ir(1)–N(1)*	95.4(3)	S(1)–V(1)–S(1)*	180.0
V(1)–S(1)	2.436(3)	S(1)–Ir(1)–N(1)*	176.7(3)	Ir(1)–S(1)–V(1)	71.44(8)	S(1)–V(1)–S(1)*	86.7(1)
Ir(2)–S(2)	2.333(4)	S(2)–Ir(2)–N(2)	84.4(4)	S(2)–Ir(2)–S(2)*	92.4(1)	S(2)–V(2)–S(2)*	92.8(1)
Ir(2)–N(2)	2.09(1)	S(2)–Ir(2)–N(2)*	89.8(4)	N(2)–Ir(2)–N(2)*	93.5(5)	S(2)–V(2)–S(2)*	180.0
V(2)–S(2)	2.442(4)	S(2)–Ir(2)–N(2)*	176.2(4)	Ir(2)–S(2)–V(2)	70.79(10)	S(2)–V(2)–S(2)*	87.2(1)

**Scheme 1**

complexes $[V^{III}\{M(aet)_3\}_2]^{3+}$ ($M = Rh^{III}$ **1**, Ir^{III} **2**) in accordance with Scheme 1. However, the reaction with half an equivalent of VCl_3 did not lead to the corresponding trinuclear complexes but instead to unidentified materials, suggesting a weak affinity between the sulfur atoms and $V(III)$ ion. This indicates that the yields of the trinuclear complexes are increased by driving the equilibrium position of the formation reaction to the right as a result of the presence of an excess of metal ions, as observed in the corresponding $[Cr^{III}\{M(aet)_3\}_2]^{3+}$ complexes.⁷ Required amounts of $V(III)$ ion for isolation of the trinuclear complexes were *ca.* 4 equivalents for **1** and *ca.* 2 equivalents for **2**. This implies that the Ir complex **2** is more easily formed or less readily decomposed in comparison with the Rh complex **1**.

The reaction of $fac(S)-[Ir(aet)_3]$ with an excess of $VOCl_2$ also leads to **2**. From ion-exchange column chromatography and absorption spectra, it was found that the known dinuclear complex $[Ir_2(aet)_4(cysta)]^{2+}$ (*cysta* = cystamine)^{16,17} containing a coordinated disulfide bond was also formed during this reaction. This indicates that the $V(IV)$ ion in $VOCl_2$ is reduced to $V(III)$ by the oxidation of some thiolato-sulfur atoms in $fac(S)-[Ir(aet)_3]$. On the other hand, a similar reaction with $fac(S)-[Rh(aet)_3]$ did not lead to **1**. The formation of **1** seems to be more difficult than that of **2** since $fac(S)-[Rh(aet)_3]$ has a lower reactivity to form the dinuclear disulfide complex compared to $fac(S)-[Ir(aet)_3]$.¹⁷

X-Ray structural analysis indicated that both the Rh complex **1** and the Ir complex **2** adopt a *meso* ($\Delta\Lambda$) configuration (*vide infra*). The formation of this *meso* form (**1a** and **2a**) in crystals may be due to the difference of solubility, since the calculated structural energies (MM2 calculation) indicate little difference between the *meso* and *rac* ($\Delta\Delta/\Lambda\Lambda$) isomers of $[M'\{M(aet)_3\}_2]^{n+}$ type complexes. The isolation of the *rac* isomers (**1b** and **2b**) was unsuccessful because of their higher solubility and instability. However, using the optically active starting material Λ - $fac(S)-[Rh(aet)_3]$, $\Delta\Lambda$ -[V{Rh(aet)₃}₂]³⁺ ($\Delta\Lambda$ -**1b**) was selectively obtained as the reaction product. Consequently, we could investigate some spectrochemical properties of both the *meso* and *rac* isomers for the Rh complex by using $\Delta\Lambda$ -**1b** as well as **1a**.

**Fig. 1** Perspective view of one of two $\Delta\Lambda$ -[V{Rh(aet)₃}₂]³⁺ (**1a**) complex cations with numbering scheme and 50% probability ellipsoids. The H-atoms are omitted for clarity. The numbering scheme of $\Delta\Lambda$ -[V{Ir(aet)₃}₂]³⁺ (**2a**) is the same as that of **1a**.

X-Ray crystal structures

For each of the dark red (**1a**(ClO₄)₃) and deep purple (**2a**(ClO₄)₃) crystals, there are two crystallographically independent complex molecules in the asymmetric unit. Since their shapes and sizes resemble each other, a perspective drawing of the complex cation of **1a** is only shown in Fig. 1 with selected bond distances and angles listed in Table 1. Both complex cations **1a** and **2a** consist of two $fac(S)-[M(aet)_3]$ ($M = Rh^{III}$ **1a**, Ir^{III} **2a**) units and one V atom. This is consistent with the plasma emission spectral analysis, which gave a value of $V : M = 1 : 2$. The presence of three perchlorates for each complex cation implies that the V atom is trivalent, and the formulation as $[V\{M(aet)_3\}_2](ClO_4)_3$ is in good agreement with the results of elemental analyses. All the aet ligands coordinate to metal atoms (M(1) and M(2)), forming approximately octahedral $fac(S)-[M(aet)_3]$ units. This suggests that the terminal $fac(S)-[M(aet)_3]$ units retain their mononuclear structure during the reaction. All the thiolato-sulfur atoms in the terminal units coordinate to the central vanadium atoms (V(1) and V(2)), forming a $V^{III}S_6$ chromophore.

For the terminal $fac(S)-[M(aet)_3]$ units in **1a** and **2a**, two optical isomers (Δ and Λ) are possible with respect to the chirality arising from the skewed pair of chelate rings. For the six bridging sulfur atoms, two chiral configurations (*R* and *S*) are possible. X-Ray crystal structural analysis shows that the two terminal $fac(S)-[M(aet)_3]$ units for **1a** or **2a** have Δ and Λ configurations, which form a *meso* structure with the crystallographic inversion center located on the central vanadium atom. The sulfur atoms selectively adopt the *R* configuration for the Δ - $fac(S)-[M(aet)_3]$ unit and the *S* one for the Λ unit, as observed in reported trinuclear complexes.^{7–11}

Table 2 IR spectral data for $\Delta\Lambda$ -[V{Rh(aet)₃}₂](ClO₄)₃ (**1a**(ClO₄)₃), $\Lambda\Lambda$ -[V{Rh(aet)₃}₂]Br₃ ($\Lambda\Lambda$ -**1b**Br₃) and $\Delta\Lambda$ -[V{Ir(aet)₃}₂](ClO₄)₃ (**2a**(ClO₄)₃)

Complexes	Peak (ν/cm^{-1}) ^a
1a	3430s, 3252s, 3114s, 2924m, 1583m, 1455w, 1421w, 1302w, 1272w, 1231w, 1144m, 1109vs, 1091vs, 978m, 920w, 844w, 710w, 661w, 627s, 521w
$\Lambda\Lambda$ - 1b	3392s, 3177s, 3091s, 2946w, 1578s, 1446w, 1417m, 1306w, 1268m, 1230w, 1141m, 1032m, 976m, 916w, 839w, 738w, 659m, 524w, 457w
2a	3432s, 3243s, 3108s, 2928w, 1577m, 1455w, 1421w, 1309w, 1272w, 1237w, 1144m, 1120vs, 1091vs, 980m, 920w, 842w, 733w, 661w, 627s, 531w

^a vs = Very strong; s = strong; m = medium; w = weak.

The overall structures of **1a** and **2a** are similar to those of the corresponding trinuclear complexes $[\text{M}'\{\text{M}(\text{aet})_3\}_2]^{n+}$ ($\text{M} = \text{Rh}^{\text{III}}$, Ir^{III} ; $\text{M}' = \text{Cr}^{\text{III}}$,⁷ Mo^{III} ,⁸ Mo^{IV} ,⁸ Re^{III} ,⁹ Co^{III} ,¹⁰ Ni^{II}),¹¹ which have been determined so far. The V–S distances (average 2.42(1) Å for **1a**, 2.439(4) Å for **2a**) are relatively long, lying at the long end of the range of the corresponding M'–S bond distances (average 2.297(2)–2.458(7) Å), which depend on M'.^{7–11} The V–S distances in **1a** and **2a** are similar to the corresponding V–S(bridged) distances in $[\text{V}_3\text{Cl}_6(\text{edt})_3]^{3-}$ (edt = ethane-1,2-dithiolate; average 2.408(11) Å), which is a rare example containing the $\text{V}^{\text{III}}\text{S}_6$ chromophore.¹⁸ Complex **2a** has somewhat longer V–S bonds than **1a**. This seems to be caused by stronger affinity of iridium toward sulfur atoms than that of rhodium. In addition, the $\text{Ir} \cdots \text{V}$ distances in **2a** (average 2.7754(8) Å) are shorter than the $\text{Rh} \cdots \text{V}$ distances in **1a** (average 2.830(1) Å). This behavior corresponds to the behavior of the Cr–S and $\text{M} \cdots \text{Cr}$ distances in $\Delta\Lambda$ -[Cr{M(aet)₃}₂]³⁺ ($\text{M} = \text{Rh}^{\text{III}}$, Ir^{III}).⁷ The $\text{M} \cdots \text{V}$ distances in **1a** and **2a** are significantly shorter than the $\text{M} \cdots \text{Cr}$ distances ($\text{M} = \text{Ir}^{\text{III}}$, 2.9096(3) Å and Rh^{III} , 2.9328(2) Å) in the Cr(III) complexes, although the V–S distances are similar to the Cr–S distances ($\text{M} = \text{Ir}^{\text{III}}$, 2.421(2) Å and Rh^{III} , 2.4110(8) Å).⁷ These facts indicate that the terminal *fac*(S)-[M(aet)₃] units are strongly attracted by the central vanadium ion. On the other hand, the M–S distances (average 2.32(2) Å for **1a**, and 2.330(4) Å for **2a**) are in good agreement with those in the corresponding complexes $[\text{M}'\{\text{M}(\text{aet})_3\}_2]^{n+}$ (averages 2.307(2)–2.341(7) Å).^{7–11} These facts suggest that the difference in the terminal units *fac*(S)-[M(aet)₃] does not affect the basic structure of the polynuclear complexes, which are mainly dependent on the nature of the central metal atoms.

Spectrochemical characterization

Major IR peaks of the obtained complexes $\Delta\Lambda$ -[V^{III}-{M(aet)₃}₂]³⁺ ($\text{M} = \text{Rh}^{\text{III}}$ **1a**, Ir^{III} **2a**) and $(-)^{\text{CD}}_{360}$ -**1b** are listed in Table 2. The IR spectral patterns for the complexes are similar to each other, reflecting the similarity in overall structure. For particular, it seems that $(-)^{\text{CD}}_{360}$ -**1b** is an S-bridged trinuclear complex similar to **1a** and **2a**, whose structures were determined by X-ray structural analysis. The IR spectral bands due to the vibration of the NH₂ group appear in the region of 3400 cm⁻¹ and those of the CH₂ group appear in the region of 3000 cm⁻¹. Bands due to the bending mode are observed in the region around 1600 cm⁻¹ for the NH₂ group and 1400 and 1300 cm⁻¹ for the CH₂ group. A strong band at 1091 cm⁻¹ for **1a** and **2a** is due to the perchlorate anion,¹⁹ and no corresponding band is observed in $(-)^{\text{CD}}_{360}$ -**1b** obtained as a bromide salt. Additionally, in comparison with the *fac*(S)-[M(aet)₃] and the corresponding trinuclear complexes $[\text{M}'\{\text{M}(\text{aet})_3\}_2]^{n+}$ ($\text{M} = \text{Rh}^{\text{III}}$, Ir^{III} ; $\text{M}' = \text{Mo}^{\text{III}}$, Mo^{IV} , Re^{III} , Co^{III}),^{8,9} the IR spectra of the present complexes showed a good match over the whole region. This also supports the fact that the terminal units retain their structure during the reaction.

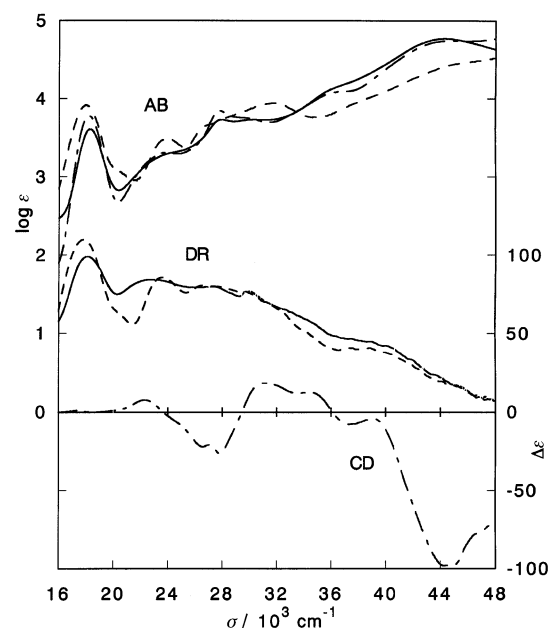


Fig. 2 UV-VIS absorption ($\log \epsilon$), diffuse reflectance (arbitrary scale) and CD spectra ($\Delta\epsilon$) of $\Delta\Lambda$ -[V{Rh(aet)₃}₂]³⁺ (**1a**; —), $\Lambda\Lambda$ -[V{Rh(aet)₃}₂]³⁺ ($\Lambda\Lambda$ -**1b**; ---) and $\Delta\Lambda$ -[V{Ir(aet)₃}₂]³⁺ (**2a**; -.-).

For both **1a** and **2a**, the UV-VIS absorption spectral patterns in aqueous solution are similar to the diffuse reflectance spectra in the solid state over the visible region (Fig. 2). This indicates that the trinuclear structures of **1a** and **2a** are retained in the solution. The UV-VIS absorption spectrum of $(-)^{\text{CD}}_{360}$ -**1b** is almost coincident with that of **1a** over the whole region (Fig. 2). Further, the CD spectral behavior of $(-)^{\text{CD}}_{360}$ -**1b** is in agreement with that of $\Delta\Lambda$ -[Re{Rh(aet)₃}₂]³⁺ over the whole region.⁹ Accordingly, $(-)^{\text{CD}}_{360}$ -**1b** can be assigned to $\Delta\Lambda$ -[V{Rh(aet)₃}₂]³⁺ ($\Lambda\Lambda$ -**1b**). As in the case of similar reactions, the absolute configuration of *fac*(S)-[Rh(aet)₃] is retained during these reactions.^{9,11}

The most intense bands at *ca.* 37 and 43 × 10³ cm⁻¹ of the Rh complexes **1a** and **1b** are characterized as due to sulfur-to-metal charge transfer (SMCT) transitions, as observed in the complexes involving *fac*(S)-[Rh(aet)₃] units.^{7–9,11–15} The bands in the region of 25–35 × 10³ cm⁻¹ can be assigned to d–d transitions, although the band at the lower energy side exhibits different behavior from those of the complexes with the *fac*(S)-[Rh(aet)₃] units. A similar absorption spectral behavior is also observed for the Ir complex **2a**, although all bands of **2a** are shifted about 5–7 × 10³ cm⁻¹ to higher energy than those of **1a**. In the visible region at < 28 × 10³ cm⁻¹, absorption and CD bands appear in **1a**, $\Lambda\Lambda$ -**1b** and **2a** (Fig. 2). Considering that the complexes with the *fac*(S)-[M(aet)₃] ($\text{M} = \text{Rh}^{\text{III}}$, Ir^{III}) units show little absorption in this region,^{7–15} these bands of **1a**, $\Lambda\Lambda$ -**1b** and **2a** can be assigned as arising from the central $\text{V}^{\text{III}}\text{S}_6$ chromophore. The extinction coefficients of these absorption bands due to the $\text{V}^{\text{III}}\text{S}_6$ chromophore are commonly > 10³ dm³ mol⁻¹ cm⁻¹, suggesting that these bands are dominated by SMCT transitions. Moreover, the intense bands around 18 × 10³ cm⁻¹ have a significant intensity. The intensity of this band in the Ir complex **2a** ($\log \epsilon = 3.92$ mol⁻¹ dm³ cm⁻¹) is greater than those of the Rh complexes **1a** ($\log \epsilon = 3.65$) and $\Lambda\Lambda$ -**1b** ($\log \epsilon = 3.78$), although the energy levels of these bands are almost the same (Fig. 2). This spectral behavior is not observed in the corresponding complexes containing other central metal ions such as Cr(III)⁷ or Co(III).^{10,12} Therefore, it is noted especially that these are the characteristic bands for polynuclear complexes containing a central V(III) ion with bridged sulfur atoms. Although all of the complexes show an intense absorption band at *ca.* 18 × 10³ cm⁻¹, the intensity of the corresponding CD band of $\Lambda\Lambda$ -**1b** is very weak. This seems to indicate that the characteristic absorption bands are optically inactive.

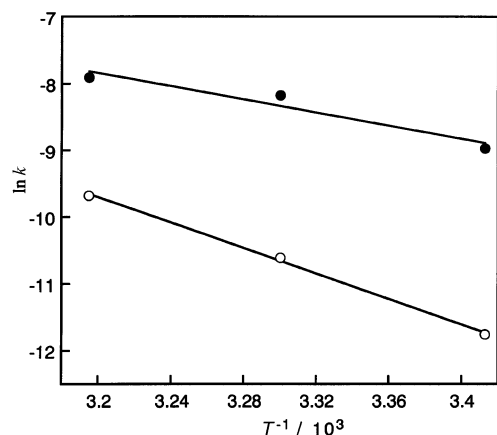


Fig. 3 Plots for activation energies of $\Delta\Lambda$ -[V{Rh(aet)₃}₂]³⁺ (**1a**; ●) and $\Delta\Lambda$ -[V{Ir(aet)₃}₂]³⁺ (**2a**; ○).

Stability and reactivity

The present trinuclear complexes in the solid state are stable even under aerobic conditions. However, some decrease of UV-VIS absorption bands, indicating decomposition of the complexes with time, was observed in solution. The decomposition of the complexes seems to be dominated by cleavage of V–S bonds, since the *fac*(S)-[M(aet)₃] (M = Rh^{III}, Ir^{III}) units are fairly stable. Indeed, *fac*(S)-[Rh(aet)₃] was deposited as a yellow powder from an aqueous solution of **1a** or $\Delta\Lambda$ -**1b** after 1 d. Moreover, taking into account that the metalloligands show weak absorption in the visible region as described above, the stability and reactivity of the present trinuclear complexes can be estimated by monitoring the characteristic band of the central V^{III}S₆ chromophore. In order to evaluate the rate of the decomposition in aqueous solution for the complexes, spectral changes of **1a** and **2a** vs. time were measured at 548.5 and 556.0 nm (18.23 and 17.99×10^3 cm⁻¹), respectively. As a result, both **1a** and **2a** decompose in a first order process taking at least several hours with the rate ($k = -\ln(A/A_0)/t$) of decomposition at 20 °C for **1a** being 1.27×10^{-4} s⁻¹ and that for **2a** being 7.85×10^{-6} s⁻¹. Considering the structures of both complexes, the V–S bonds are somewhat longer in **2a** indicating a weaker bond strength than **1a**. However, **2a** was more stable in aqueous solution than **1a**. This suggests that the V–S bond length is not the major factor which determines the stability in aqueous solution. Further, similar measurements at 30 and 40 °C were carried out. From these measurements it was found that the calculated activation energies E_a for **1a** and **2a** were 40.9 and 79.1 kJ mol⁻¹, respectively (Fig. 3). This result indicates that **2a** is more stable to decomposition than **1a**. In the known trinuclear complexes [M′{M(aet)₃}₂]ⁿ⁺ (M = Rh^{III}, Ir^{III}; M′ = Cr^{III}, Co^{III}),^{7,10} a stronger Ir–S bond compared to the Rh–S bond is observed and is directly attributed to the bond strength of the M′–S bond. The trinuclear complexes [M′{Ir(aet)₃}₂] have a tendency to contain weaker M′–S bonds as opposed to the corresponding Rh(III) complexes.^{7,10} Thus, *fac*(S)-[Ir(aet)₃], which has stronger Ir–S bonds is a ‘poorer’ terminal unit than *fac*(S)-[Rh(aet)₃] which has weaker Rh–S bonds. However, as described above, **2a** is considerably more stable than **1a** in aqueous solution, despite weaker V–S bonds. This is the first example of trinuclear complexes with terminal *fac*(S)-[Ir(aet)₃] units, being more stable than that with the *fac*(S)-[Rh(aet)₃] units. This unusual behavior of **2a** may be due to a metal–metal interaction *via* direct metal orbital–metal orbital overlapping.^{20,21}

Metal exchange reactions of the central V(III) atom in the Rh complex **1a** using 1 equivalent of NiCl₂ or CoCl₂ were attempted (Scheme 2). As shown in Fig. 4, the absorption spectral change of **1a** upon reaction with Ni(II) ion was observed with three isosbestic points at 372, 514 and 596 nm. The characteristic band around 406 nm (24.6×10^3 cm⁻¹) for

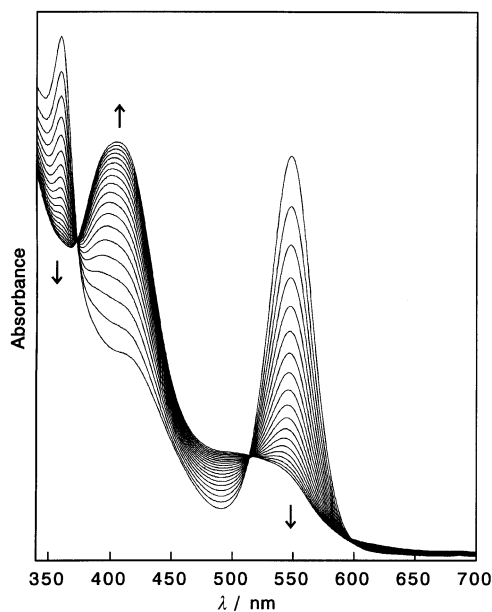
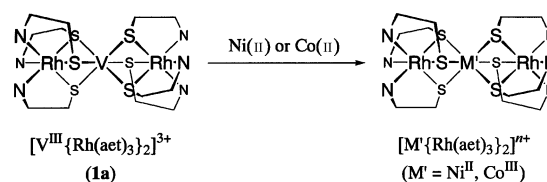


Fig. 4 Absorption spectral change of $\Delta\Lambda$ -[V{Rh(aet)₃}₂]³⁺ (**1a**) upon addition of Ni(II); the curves show the spectra measured at 5 min intervals.



Scheme 2

[Ni{Rh(aet)₃}₂]²⁺¹¹ increases in intensity with time and the band around 550 nm (18.2×10^3 cm⁻¹), which is due to the V^{III}S₆ chromophore for **1a**, decreases in intensity. This indicates that **1a** is undergoing a metal exchange reaction. The rate of formation of [Ni{Rh(aet)₃}₂]²⁺ from the reaction of [V{Rh(aet)₃}₂]³⁺ with NiCl₂ (1 : 1 molar ratio), calculated using the equation $\ln(A_{t+\tau} - A_t) = -kt + \text{Constant}$, where A_t denotes the absorbance at time t s and $A_{t+\tau}$ denotes the absorbance at time $(t + \tau)$ s, is 5.10×10^{-4} s⁻¹. Analogous results were obtained when this reaction was attempted by using Co(II) ion instead of Ni(II) ion. As the reaction proceeds, the band around 550 nm of **1a** decreases, whereas a new band, which is thought to be a d–d band for [Co{Rh(aet)₃}₂]³⁺,¹² appeared at 540.5 nm (Fig. S1 of electronic supplementary information).† The rate of formation for [Co{Rh(aet)₃}₂]³⁺ from the reaction of [V{Rh(aet)₃}₂]³⁺ with CoCl₂ (1 : 1 molar ratio) is 1.81×10^{-4} s⁻¹. Since the formation of the [Co{Rh(aet)₃}₂]³⁺ requires oxidation of Co(II) to Co(III), direct synthesis was attempted by using [Co^{III}(NH₃)₅(H₂O)]³⁺ instead of Co^{II}Cl₂. Acceleration in the rate of formation was observed in this reaction, indicating that the oxidation of Co(II) to Co(III) is the rate determining step for the formation of [Co{Rh(aet)₃}₂]³⁺ from [V{Rh(aet)₃}₂]³⁺. The Ni(II) and Co(II) ions quantitatively form the trinuclear complexes upon reaction with *fac*(S)-[Rh(aet)₃].¹³ The present metal exchange reaction reflects the weak affinity of V(III) ion toward thiolato-sulfur atoms.

Redox and magnetic properties

As shown in Fig. 5, the cyclic voltammograms for **1a** and **2a** display some irreversible oxidation or reduction waves in both the positive and negative potential regions. The irreversible reduction wave ($E_{pc} = -0.85$ V for **1a** and $E_{pc} = -0.88$ V for **2a** vs. Ag/AgCl) probably involves a V^{III/II} reduction process, since the terminal *fac*(S)-[Rh(aet)₃] or *fac*(S)-[Ir(aet)₃] unit does not undergo a Rh^{III/II} or Ir^{III/II} redox process in the potential region

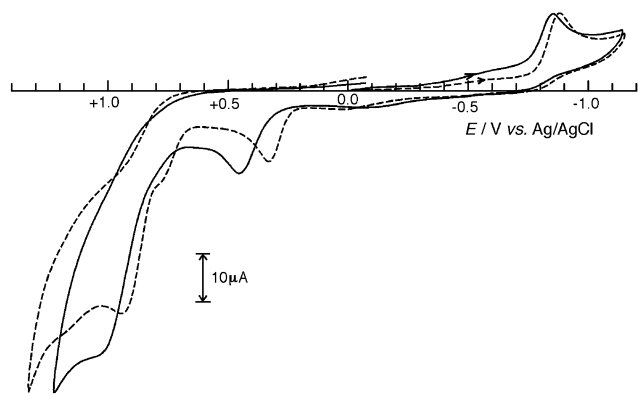


Fig. 5 Cyclic voltammograms of $\Delta\Lambda$ -[V{Rh(aet)₃]₂]³⁺ (**1a**; —) and $\Delta\Lambda$ -[V{Ir(aet)₃]₂]³⁺ (**2a**; ---); scan rate 100 mV s⁻¹.

of >-1.1 V.^{7,10} This behavior is similar to that of Cr^{III} reduction in [Cr^{III}{M(aet)₃]₂]³⁺ ($E_{pc} = -0.86$ V for the Rh complex and $E_{pc} = -0.85$ V for the Ir complex).⁷ The observation that the irreversible V^{III} or Cr^{III} reduction waves in the Rh and Ir complexes appeared at almost the same potential, is different from the observation that the reversible Co^{III} redox couples in [Co^{III}{M(aet)₃]₂]³⁺ appeared at distinctly different potentials ($E^0 = -0.36$ V for the Rh complex and $E^0 = -0.23$ V for the Ir complex).¹⁰ Thus, the central V(III) ions in [V^{III}{Rh^{III}(aet)₃]₂]³⁺ and [V^{III}{Ir^{III}(aet)₃]₂]³⁺ are reduced at fairly negative potentials which are independent of the nature of the terminal units. The oxidation waves ($E_{pa} = +0.45$ V for **1a** and $E_{pa} = +0.33$ V for **2a**) were not observed unless going through the reduction scans. [M₂(aet)₄(cysta)₂]²⁺ (M = Rh^{III}, Ir^{III}) also show oxidation waves, which are thought to be due to oxidation of the Rh or Ir center in the mononuclear unit formed by reductive decomposition of the dinuclear complexes, in the corresponding region.¹⁷ This seems to indicate that the wave at ca. +0.4 V can be defined as arising from complexes formed after decomposition. The waves observed at $E_{pa} = +1.04$ V for **1a** and +0.94 V for **2a** are thought to be dominated by a V^{III}/V^{IV} oxidation process. For **2a**, the wave at +0.75 V, which appears to be due to the terminal *fac*(S)-[Ir(aet)₃] units, was observed as a shoulder. However, reversible redox couples as seen for the corresponding complexes [M'^{III}{M(aet)₃]₂]³⁺ (M = Rh^{III}, Ir^{III}, M' = Cr^{III}, Co^{III})^{7,10} were not observed.

Although the magnetic moment of the Rh complex **1a** (2.59 μ_B) at room temperature is somewhat lower than that expected from the central V(III) ion, which has a d² electronic structure, it is in agreement with those of mononuclear V(III) complexes containing tris(2-thiolatoethyl)amine (2.53–2.91 μ_B)²² or 1,4,7-trithiacyclononane as ligands (2.55–2.80 μ_B).²³ However, Ir complex **2a** exhibited an even lower magnetic moment (2.27 μ_B). This behavior is inconsistent with the fact that the corresponding trinuclear Rh and Ir complexes containing the Cr(III) ion, [Cr{M(aet)₃]₂]³⁺ (M = Rh^{III}, Ir^{III}), show magnetic moments expected from the spin-only value for the d³ configuration.⁷ On the other hand, the corresponding Rh complexes containing Mo(III) or Re(III), [M'^{III}{Rh(aet)₃]₂]³⁺ (M' = Mo^{III} or Re^{III}), show lower magnetic moments than the spin-only value for the d³ or d⁴ configuration.^{8,9} Accordingly, the magnetic behavior at room temperature of the linear-type S-bridged trinuclear complexes indicate diagonal similarity of the central early transition metal ions. These low magnetic moments might be related to a partly low-spin arrangement of unpaired electrons.

Experimental

Materials

2-Aminoethanethiol (Haet), RhCl₃·*n*H₂O and IrCl₃ were purchased from Tokyo Kasei Kogyo Co. Ltd., N. E. Chemcat

Co. Ltd. and Rare metallic Co. Ltd., respectively. Na₂[Sb₂(*R,R*-tart)₂]·5H₂O (H₄tart = tartaric acid) was prepared by the general procedure from Na₂(*R,R*-H₃tartrato)₂·H₂O and Sb₂O₃. The mononuclear complexes, *fac*(S)-[Rh(aet)₃]³⁺^{7,14,24} and *fac*(S)-[Ir(aet)₃]³⁺^{7,10} were prepared from the reactions of RhCl₃·*n*H₂O or IrCl₃ with a large excess of Haet by procedures similar to those in the literature. Optically active Λ -*fac*(S)-[Rh(aet)₃]³⁺¹³ was obtained from the capture reaction with ethylenediaminetetraacetic acid of Zn(II) of the heptanuclear complex $\Lambda\Lambda\Lambda\Lambda$ -[Rh(aet)₃]₄Zn₃OHBr₅,¹⁵ which was resolved using Na₂[Sb₂(*R,R*-tart)₂]·5H₂O instead of K₂[Sb₂(*R,R*-tart)₂]·3H₂O. The other reagents were purchased from Wako Pure Chemical Ind. Co. Ltd. or Kanto Chemical Ind. Co. Ltd. All chemicals were used without further purification.

Preparation of polynuclear complexes

CAUTION: perchlorate compounds are potentially explosive. Therefore, these must be handled with great care.

$\Delta\Lambda$ -[V{Rh(aet)₃]₂]³⁺ **1a.** A suspension containing *fac*(S)-[Rh(aet)₃] (0.20 g, 0.60 mmol) and VCl₃ (0.38 g, 2.4 mmol) in 20 cm³ of H₂O, which was deoxygenated by bubbling nitrogen gas for 1 h, was gradually heated to 50 °C and stirred for 1 h and the mixture turned dark red. A small amount of unreacted materials were removed and five drops of saturated NaClO₄ solution were then added to the filtrate. The solution was allowed to stand in a glove-box overnight and dark red crystals of **1a**(ClO₄)₃ were collected by filtration and washed with a small amount of water, methanol, ethanol and acetone. Anal. Found: C, 14.53; H, 3.63; N, 8.05; Rh, 20.42; V, 4.89%. [V{Rh(C₂H₆NS)₃]₂](ClO₄)₃ requires C, 14.24; H, 3.59; N, 8.31; Rh, 20.34; V, 5.03%.

$\Delta\Lambda$ -[V{Rh(aet)₃]₂]³⁺ (–)₃₆₀-1b**.** A suspension containing Λ -*fac*(S)-[Rh(aet)₃] (0.080 g, 0.24 mmol) and VCl₃ (0.15 g, 0.95 mmol) in 8 cm³ of deoxygenated H₂O was gradually heated to 50 °C and stirred for 1 h, whereupon it became a dark red solution. A small amount of unreacted materials were removed and 1 cm³ of saturated NaBr solution was then added to the filtrate. The solution was allowed to stand in a refrigerator overnight and dark red microcrystals of (–)₃₆₀-**1b**Br₃ were collected by filtration and washed with a small amount of water, methanol, ethanol and acetone. Anal. Found: C, 14.42; H, 4.26; N, 8.42%. [V{Rh(C₂H₆NS)₃]₂Br₃·3H₂O requires C, 14.31; H, 4.20; N, 8.34%.

$\Delta\Lambda$ -[V{Ir(aet)₃]₂]³⁺ **2a. Method 1.** To a suspension containing *fac*(S)-[Ir(aet)₃] (0.20 g, 0.48 mmol) in 30 cm³ of H₂O was added VCl₃ (0.15 g, 1.0 mmol). The mixture was gradually heated to 60 °C and stirred for 1 h, whereupon it became a deep purple solution. A small amount of unreacted materials were removed and five drops of saturated NaClO₄ solution were added to the filtrate. The solution was allowed to stand in a vacuum desiccator for 2 weeks. The resulting deep purple crystals of **2a**(ClO₄)₃ were collected by filtration and washed with a small amount of water, methanol, ethanol and acetone.

Method 2. To a suspension containing *fac*(S)-[Ir(aet)₃] (0.20 g, 0.48 mmol) in 30 cm³ of H₂O was added VOCl₂ (0.26 g, 1.9 mmol). The temperature of the mixture was gradually increased to 60 °C. After stirring at 60 °C overnight, the mixture turned deep purple. A small amount of unreacted *fac*(S)-[Ir(aet)₃] was filtered off and 10 drops of saturated NaClO₄ solution were added to the solution followed by storing in a refrigerator overnight. The resulting purple powder of **2a**(ClO₄)₃ was filtered off and washed with methanol, ethanol and acetone. Anal. Found: C, 12.16; H, 3.18; N, 7.01%. [V{Ir(C₂H₆NS)₃]₂](ClO₄)₃ requires C, 12.11; H, 3.04; N, 7.06%.

Measurements

Elemental analysis (C, H, N) were performed by the Analysis

Table 3 Crystallographic data for $\Delta\Delta$ -[V{Rh(aet)₃]₂](ClO₄)₃ (**1a**(ClO₄)₃) and $\Delta\Delta$ -[V{Ir(aet)₃]₂](ClO₄)₃ (**2a**(ClO₄)₃)

	1a (ClO ₄) ₃	2a (ClO ₄) ₃
Chemical formula	C ₁₂ H ₃₆ N ₆ O ₁₂ S ₆ Rh ₂ V	C ₁₂ H ₃₆ N ₆ O ₁₂ S ₆ Ir ₂ V
Formula weight	1011.92	1190.53
Crystal system	Trigonal	Trigonal
Space group	<i>R</i> $\bar{3}$ (no. 148)	<i>R</i> $\bar{3}$ (no. 148)
<i>a</i> /Å	14.517(4)	14.578(9)
<i>c</i> /Å	26.680(5)	26.47(2)
<i>V</i> /Å ³	4869(1)	4871(4)
<i>Z</i>	6	6
<i>D</i> _c /g cm ⁻³	2.070	2.435
μ /mm ⁻¹	1.978	9.173
Collected reflections	2684	8088
Unique reflections	2683	7727
<i>R</i> _{int}	0.018	0.073
Observations (<i>I</i> > 1.5σ(<i>I</i>))	1489	1438
Variable parameters	164	129
<i>R</i> ; <i>R</i> _w	0.049; 0.070	0.045; 0.047
GOF	1.30	1.36

^a $R = \sum ||F_o| - |F_c|| / \sum |F_o|$; $R_w = [\sum w(|F_o| - |F_c|)^2 / \sum w F_o^2]^{1/2}$, $w = 1/\sigma^2 |F_o|$.

Center of the University of Tsukuba. The concentrations of V and Rh in the complexes were determined with a NIPPON Jarrell-Ash ICPA-575 ICP spectrophotometer. UV-VIS absorption spectra were recorded with a JASCO V-560 or a V-570 spectrophotometer and diffuse reflectance spectra were recorded on a JASCO V-570 spectrophotometer equipped with an integrating sphere apparatus. CD spectra were recorded with a JASCO J-600 spectropolarimeter. IR spectra were recorded with a JASCO FT/IR-550 spectrophotometer using KBr disks in the range 4000–400 cm⁻¹. Magnetic susceptibilities were measured with a Sherwood Scientific susceptibility balance (MSB-AUTO) at room temperature with diamagnetic corrections obtained employing tabulated constants.²⁵ Electrochemical measurements were conducted using a CV-1B apparatus (Bioanalytical systems (BAS)), using a glassy carbon working electrode (BAS, GCE). An aqueous Ag/AgCl/NaCl (3 mol dm⁻³) electrode (BAS, RE-1) and platinum wire were used as reference and auxiliary electrodes, respectively. Electrochemical experiments were conducted in a 0.1 mol dm⁻³ aqueous solution of Na₂SO₄ as supporting electrolyte and employing complex concentrations of 1.0 mmol dm⁻³. Molecular Mechanics (MM2) calculations were performed by a Power Macintosh computer 6100/60 with CAChe program.²⁶

Absorption spectral changes for aqueous solutions containing 0.4 mmol dm⁻³ of **1a** or 0.2 mmol dm⁻³ of **2a** were measured at 20, 30 and 40 °C on the JASCO V-570 spectrophotometer equipped with a Peltier type thermostatic cell holder (JASCO ETC-505) and a TAIYO COOLNIT CL-19. The metal exchange reactions for aqueous solutions containing 0.4 mmol dm⁻³ of **1a** and 0.4 mmol dm⁻³ of NiCl₂ or CoCl₂ were monitored on the JASCO V-570 spectrophotometer at room temperature. The rate constants *k* and activation energies *E*_a were obtained from the slopes of linear least-squares plots.

Crystallography

Single crystals of **1a**(ClO₄)₃ and **2a**(ClO₄)₃ were used for data collection on a Rigaku AFC-7S four-circle diffractometer with graphite-monochromatized Mo-*K*α (0.71069 Å) radiation. The intensity data were collected by the ω -2 θ scan technique up to 55°. Crystal data and experimental parameters are listed in Table 3.

The positions of most non-hydrogen atoms were determined by direct methods (SIR92)²⁷ and some remaining atom positions were found by successive difference Fourier techniques. The structures were refined by full-matrix least-squares techniques using anisotropic thermal parameters for non-hydrogen atoms. All the hydrogen atoms were included in the

refinement but restrained to ride on attached atoms (C–H = N–H = 0.95 Å, *U* = 1.3 *U*(C, N)). The metal atoms (Rh, Ir, V) of both complexes were constrained to the special positions of symmetry. In complex cation **1a**, one of the two crystallographically independent molecules exhibits disorder for the chelate ring. The site occupancy factor of the S(2), N(2), C(3,4) atom sets are fixed to 5/6 and those of the S(3), N(3), C(5,6) atom sets are fixed to 1/6 as ideal values. All of the calculations were performed using the teXsan crystallographic software package.²⁸

CCDC reference numbers 160876 and 160877.

See <http://www.rsc.org/suppdata/dt/b1/b101965/> for crystallographic data in CIF or other electronic format.

Acknowledgments

This work was supported by a Grant-in-Aid for Scientific Research Nos. 12023205 and 11640555 from the Ministry of Education, Science, Sports and Culture.

References

- 1 R. R. Eady, *Chem. Rev.*, 1996, **96**, 3013 and references therein.
- 2 J. G. Reynolds and W. R. Biggs, *Acc. Chem. Res.*, 1988, **21**, 319 and references therein.
- 3 M. Henze, *Hoppe-Seyler's Z. Physiol. Chem.*, 1911, **72**, 494.
- 4 H. Michibata, T. Uyama, T. Ueki and K. Kanamori, The Mechanism of Accumulation and Reduction of Vanadium by Ascidians, in *The Biology of Ascidian*, ed. H. Sawada, H. Yokosawa and C. C. Lambert, Springer, Tokyo, 2001.
- 5 K. Kanamori, K. Yamamoto, T. Okayasu, N. Matsui, K. Okamoto and W. Mori, *Bull. Chem. Soc. Jpn.*, 1997, **70**, 3031.
- 6 K. Okamoto, C. Sasaki, Y. Yamada and T. Konno, *Bull. Chem. Soc. Jpn.*, 1999, **72**, 1685 and references therein.
- 7 Y. Miyashita, N. Sakagami, Y. Yamada, T. Konno, J. Hidaka and K. Okamoto, *Bull. Chem. Soc. Jpn.*, 1998, **71**, 661.
- 8 Y. Miyashita, Y. Yamada, K. Fujisawa, T. Konno, K. Kanamori and K. Okamoto, *J. Chem. Soc., Dalton Trans.*, 2000, 981.
- 9 Y. Miyashita, N. Mahboob, S. Tsuboi, Y. Yamada, K. Fujisawa and K. Okamoto, *Bull. Chem. Soc. Jpn.*, 2001, in press.
- 10 T. Konno, K. Nakamura, K. Okamoto and J. Hidaka, *Bull. Chem. Soc. Jpn.*, 1993, **66**, 2582.
- 11 T. Konno and K. Okamoto, *Bull. Chem. Soc. Jpn.*, 1995, **68**, 610.
- 12 T. Konno, S. Aizawa, K. Okamoto and J. Hidaka, *Bull. Chem. Soc. Jpn.*, 1990, **63**, 792.
- 13 S. Aizawa, Y. Sone, S. Yamada and M. Nakamura, *Chem. Lett.*, 1998, 775; S. Aizawa, Y. Sone, S. Khajar, Y. Ohishi, S. Yamada and M. Nakamura, *Bull. Chem. Soc. Jpn.*, 2000, **73**, 2043.
- 14 T. Konno, K. Okamoto and J. Hidaka, *Inorg. Chem.*, 1994, **33**, 538.
- 15 T. Konno, K. Okamoto and J. Hidaka, *Chem. Lett.*, 1990, 1043; T. Konno, K. Okamoto and J. Hidaka, *Bull. Chem. Soc. Jpn.*, 1994, **67**, 101.
- 16 T. Konno, Y. Miyashita and K. Okamoto, *Chem. Lett.*, 1997, 85.
- 17 Y. Miyashita, N. Sakagami, Y. Yamada, T. Konno and K. Okamoto, *Bull. Chem. Soc. Jpn.*, 1998, **71**, 2153.
- 18 R. J. Rambo, S. L. Castro, K. Folting, S. L. Bartly, R. A. Heintz and G. Christou, *Inorg. Chem.*, 1996, **35**, 6844.
- 19 K. Nakamoto, *Infrared and Raman Spectra of Inorganic and Coordination Compounds*, John Wiley & Sons, New York, 5th edn., 1997.
- 20 R. E. DeSimone, T. Onyko, L. Wardman and E. L. Blinn, *Inorg. Chem.*, 1975, **14**, 1313.
- 21 B. Albela, E. Bill, O. Brosch, T. Weyhermüller and K. Wieghardt, *Eur. J. Inorg. Chem.*, 2000, 139.
- 22 S. C. Davies, D. L. Hughes, Z. Janas, L. B. Jerzykiewicz, R. L. Richards, J. R. Sanders, J. E. Silverston and P. Sobota, *Inorg. Chem.*, 2000, **39**, 3485.
- 23 S. C. Davies, M. C. Durrant, D. L. Hughes, C. L. Floch, S. J. A. Pope, G. Reid, R. L. Richards and J. R. Sanders, *J. Chem. Soc., Dalton Trans.*, 1998, 2191.
- 24 M. Kita, K. Yamanari and Y. Shimura, *Bull. Chem. Soc. Jpn.*, 1983, **56**, 3272.
- 25 C. J. O'Connor, *Prog. Inorg. Chem.*, 1982, **29**, 203.
- 26 CAChe, Version 3.7. CAChe Scientific, Inc, Tokyo, Japan, 1994.
- 27 A. Altomare, M. C. Burla, M. Camalli, M. Casciarano, C. Giacovazzo, A. Guagliardi and G. Polidori, *J. Appl. Crystallogr.*, 1994, **27**, 435.
- 28 teXsan. Single Crystal Structure Analysis Software, Version 1.10, Molecular Structure Corporation, The Woodlands, TX, 1999.